Observation of Velocity Bunching of Near–Zone-Edge Phonons in Semiconductors: An Intense, Tunable Phonon Source near 10 Å

P. Hu, V. Narayanamurti, and M. A. Chin

Bell Laboratories, Murray Hill, New Jersey 07974

Experiments are reported on velocity bunching of near–zone-edge phonon pulses generated in the interband energy-relaxation process of photoexcited electron-hole pairs in GaAs and InP. The bunching is achieved by scanning the photoexcited region along the direction of phonon propagation at various velocities corresponding to different dispersive points on the phonon branch. This intense, tunable phonon source can be operated in the 10-Å wavelength region.

Recent time-of-flight experiments[1] by Ulbrich, Narayanamurti, and Chin have shown that the interband energy relaxation of photoexcited electron-hole pairs in bulk, high-purity samples of zinc-blende–type semiconductors such as GaAs and InP occurs via large–wave-vector transverse acoustic (TA) phonons, which were surprisingly able to propagate macroscopic distances ~ 2.5 mm in a ballistic fashion and with a shape characteristic of a dispersive medium.

In this Letter we report on a novel method of sharpening dispersive pulses in solids in a controlled fashion. This has been achieved by scanning the laser excitation region (light spot) along the direction of phonon propagation at various velocities corresponding to different dispersive points on the phonon branch. In the dispersive region, the sharp-pulse arrival time is shown to scale with the laser scanning speed and the data suggest that we have an intense, tunable, traveling-wave phonon source in the 10-Å wavelength region.

In Fig. 1(a) we show a set of phonon dispersion curves[2] for GaAs along the [111] direction. The optically excited, high-energy optical and longitudinal acoustic (LA) phonons quickly decay into long-lived TA phonons which have an extremely high density of states. The group velocity, V_{group}, of these phonons is shown in Fig. 1(b) as a function of phonon frequency ν. There is considerable dispersion in V_{group} in the frequency region of $\sim (1-2) \times 10^{12}$ Hz and for phonon wavelengths less than about 25 Å.

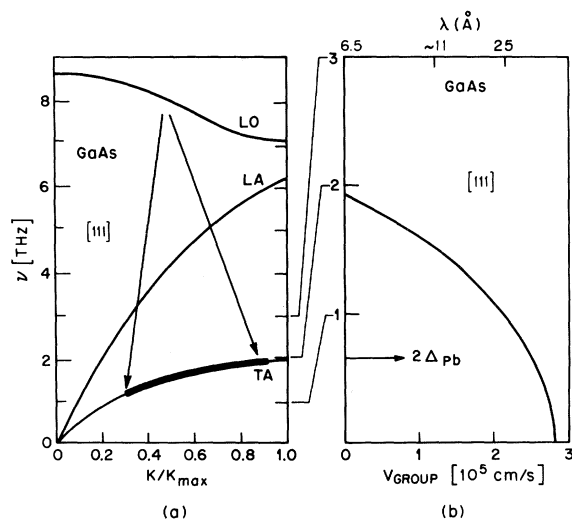The photoexcitation was done by means of a cw

FIG. 1. (a) Phonon dispersion curves for GaAs in the [111] direction. The figure shows decay scheme of optically excited LO phonons into near–zone-edge TA phonons. (b) TA-phonon group velocities as a function of phonon frequency.
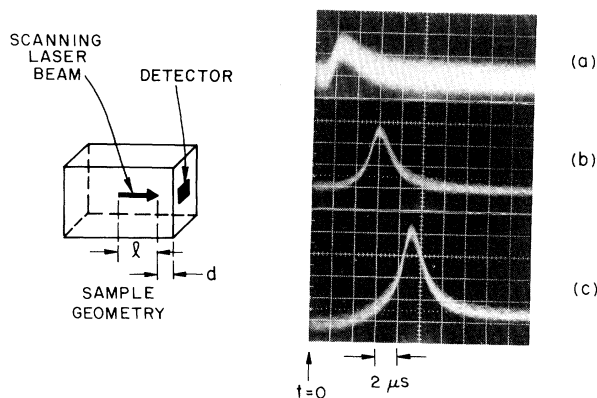

FIG. 2. Schematic on left shows the geometry of the sample. A variable-speed, spinning mirror is used for scanning the laser beam along the sample surface. The laser scanning distance is l and the free propagation distance is d. Photographs show typical pulses for three different scanning velocities: (a) 3.8×10^5, (b) 0.47×10^5, and (c) 0.286×10^5 cm/sec. Time scale is 2 μsec for each large division. The peak arrival times are (a) 2.0 ± 0.2, (b) 5.6 ± 0.2, and (c) 8.9 ± 0.2 μsec.

argon laser. The scanning of the laser beam was achieved by means of a spinning mirror which could be rotated at speeds as high as 60 000 rpm. The laser beam was focused to a spot of size ~ 100 μm. A diode was used to monitor the optical pulses. A schematic of the sample geometry is shown in Fig. 2. The detector in these experiments was either a Pb-oxide-Pb tunnel junction or a small superconducting Al bolometer of area ~ 10^{-2} mm^2. Similar results were obtained with both sets of detectors. The light impinged on the (111) sample face while the detector was evaporated within 100 μm of the 90-deg sample edge on the (211) face. A small distance ($d_0 \sim 0.42$ mm) from the detector edge was carefully masked to prevent any optical feedthrough or surface excitations from reaching the detector. The scanning distance l and free propagation distance $d = d_0 + \Delta d$ could be varied *in situ* in the experiment. The experiments were done at $T \approx 1.5$ K (in He liquid) on high-purity samples[3] of GaAs and InP. The sample surfaces were highly polished by a combined mechanical and chemical etch.

In Fig. 2, we show a few typical photographs of observed pulses for scanning velocities of 3.8 $\times10^5$, 0.47×10^5, and 0.286×10^5 cm/sec with peak arrival times of 2.0 ± 0.2, 5.6 ± 0.2, and 8.9 ± 0.2 μsec, respectively. Here the scanning distance $l \sim 2.17$ mm and $d \sim 0.42$ mm. It is clear from these photographs that the pulse arrival time and shape change markedly with scanning velocity. At high sweep speeds ($> 10^5$ cm/sec), the pulses have a long trailing edge. At intermediate sweep speeds (~ 0.6 to 0.2×10^5 cm/sec), the pulses are symmetric and, as we shall see below, have an arrival time which scales with scanning velocity. At very slow sweep speeds ($< 10^4$ cm/sec), the pulse trailing edge has a very sharp cutoff and is very sensitive to distance (see Fig. 4 below).

The propagation velocity of the generated phonons was accurately determined by monitoring the change (Δt) in peak arrival time as a function of the change (Δd) in the "free" propagation distance d. Insets (a) and (b) of Fig. 3 show a few typical plots of Δt vs Δd. The solid lines represent the actual laser scanning speeds used. The dashed line in inset (a) corresponds to the low-frequency TA ballistic velocity of 2.8×10^5 cm/sec. It is clear from this inset that at intermediate sweep speeds the phonons propagate *ballistically* for distances > 1.5 mm but with a velocity corresponding to *dispersed, high-frequency phonons* and not to low-frequency ones. At very slow

speeds ($\lesssim 10^4$ cm/sec) the pulse arrival time departs markedly from linearity for $d \gtrsim 0.5$ mm, indicating the onset of attenuation and frequency down conversion. Figure 3 also shows a plot of the observed initial phonon velocity ($\Delta d/\Delta t$) at $d = 0.67$ mm as a function of the scanning velocity. At high scanning speeds, the pulse velocity saturates at a value (~ 0.6×10^5 cm/sec) which is close to the peak velocity of the generated phonons.[1] The solid line in this figure has a slope of unity and indicates a linear tuning range of roughly one order of magnitude in velocity. This range can be extended further by going to smaller "free" propagation distances, d.

In Fig. 4 we show the amplitude behavior and the pulse shape at low velocities. The photograph is for a scanning velocity of 10^4 cm/sec and shows the sharp cutoff of the trailing edge very clearly. The amplitude and velocity of the phonons are now severely affected by attenuation. The amplitude plot of Fig. 4 is for a fixed scanning length $l = 2.2$ mm but for two different distances d of 0.42 mm and 0.75 mm. At high sweep speeds (lower phonon frequency or longer phonon wavelength) the amplitude increase is linear, but at very slow sweep speeds it levels off, again indicating the onset of attenuation. From data such
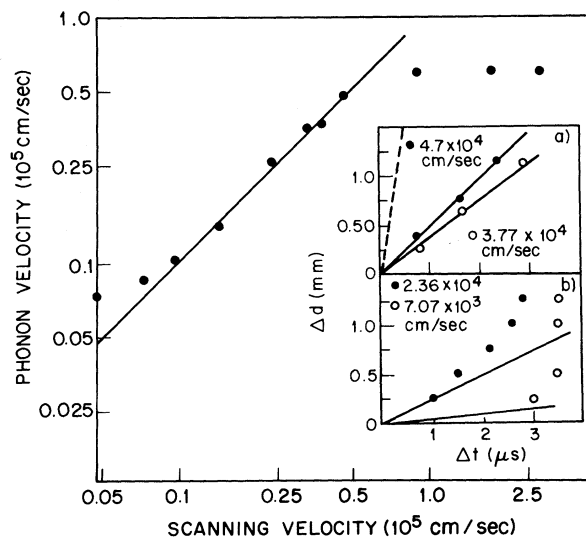
FIG. 3. Initial free-propagation phonon velocity as a function of laser scanning velocity. Straight line has slope unity. Insets (a) and (b) show the change in arrival time Δt as a function of changes in "free" propagation distance Δd. Solid lines are the appropriate laser scanning velocities. The dashed line in (a) corresponds to the low-frequency ballistic TA velocity of 2.8×10^5 cm/sec. See text.
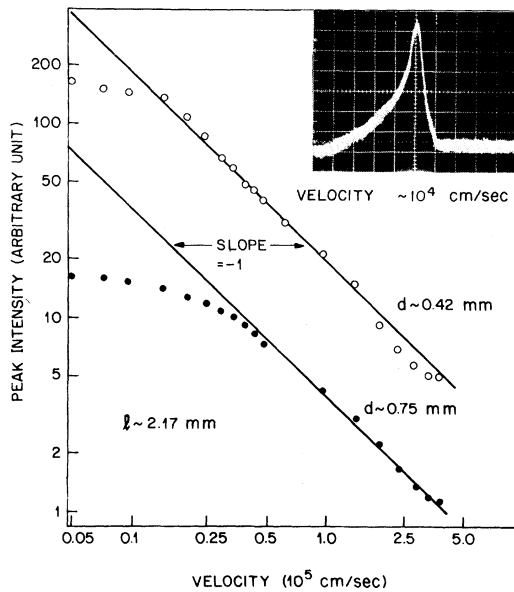
FIG. 4. Peak intensity as a function of scanning velocity for two different distances d and a fixed scanning length l of 2.17 mm. At low velocities attenuation becomes significant, as shown also in the photograph which corresponds to a scanning velocity of 10^4 cm/sec. Time scale is 5 μsec for each large division.

as these, we estimate that the mean free path of phonons with velocity $\gtrsim 5 \times 10^4$ cm/sec is ~ 2.5 mm while the very slow ones (velocity $\lesssim 10^4$ cm/sec) have a mean free path < 0.5 mm. From the velocity curves in the inset of Fig. 3 we estimate that the phonon lifetime is almost constant and ~ 3 μsec, consistent with the relatively small changes in phonon frequency in the very dispersive region. The mean free path, however, changes and gets smaller as the phonon velocity is reduced.

We would now like to mention several checks which we made on our experiment. Instead of exciting the semiconductor directly, we evaporated a 1000-Å-thick Constantan metal film and studied the phonons generated after optical excitation. We now observed ballistic phonons whose velocity (~ 2.8×10^5 cm/sec) was independent of the laser scanning speed, as is to be expected for low-frequency, nondispersive wave propagation. No tuning was possible even in the direct–semiconductor-excitation experiments if the detector was not in line with the scanning beam or if the scanning direction was opposite to the direction of phonon detection. Finally, the tuning behavior described earlier was reproduced in two different samples of GaAs and one high-quality sample of InP.

Finally, we would like to mention here that at a fixed scanning speed in the direct–semiconductor-excitation experiment the pulse amplitude scaled roughly with input laser power over the accessible range of 20 mW to 0.5 W. We have tried to model theoretically our observed pulses on a model of linear velocity bunching. This does give tuning, but a pulse width somewhat larger than we observed. Part of the shape at slow speeds is certainly modified by attenuation. It is, however, possible that a nonlinear process may also be occurring. Because of the anomalously long lifetimes of the TA phonons, this may be the case, as first theoretically proposed by Orbach.[4,5]

In summary, the observed high and low sweep cutoffs, the threshold nature of the Pb junction detector (which places a lower bound of 0.7×10^{12} Hz on the phonon frequency), the sensitivity to distance, and the scaling of the "free" propagation velocity with sweep speed in the dispersive region are consistent with the result that the phonon bunching represents a pulse with a well-defined frequency and wave vector which can be conveniently tuned by simply altering the laser scanning speed. The precise tuning range in wavelength would obviously depend in detail on the direction of propagation and the intrinsic phonon-dispersion curve. The source is intense ($\gtrsim 10^{-1}$ W/mm^2), can be operated independently of the superconducting detector, and can operate in high magnetic fields. We believe it will work in any III-V and zinc-blende–type semiconductors which have soft TA-phonon branches particularly in the [111] direction. In the event of large impurity or isotope scattering, one would simply have to move the laser spot closer to the detector and possibly work with higher excitation powers. Such a phonon source can be of great use for physical studies of solids and for phonon optics.[6]

[1]R. G. Ulbrich, V. Narayanamurti, and M. A. Chin, Phys. Rev. Lett. 45, 1432 (1980).

[2]J. T. Waugh and G. J. Dolling, Phys. Rev. 132, 2410 (1963).

[3]The samples used in this work were free (<< 0.1 ppm) of transition-metal impurities. These impurities cause considerable phonon scattering in the millielectronvolt range. See V. Narayanamurti, R. A. Logan, and M. A. Chin, Appl. Phys. Lett. 33, 481 (1978).

[4]R. Orbach, Phys. Rev. Lett. 16, 15 (1966).

[5]R. Orbach, IEEE Trans. Sonics Ultrason. 14, 140 (1967). Typical calculated power densities for stimulated processes to occur are estimated to be $\sim(10-100)$ W/cm^3 while typical experimental power densities are $\sim(10^4-10^6)$ W/cm^3.

[6]For a recent review, see V. Narayanamurti, in *Proceedings of NATO Advanced Study Institute on Non-Equilibrium Superconductivity, Phonons and Kapitza Boundaries*, edited by K. E. Gray (Plenum, New York, 1980).

Zero-Field Hyperfine Resonance of Atomic Hydrogen for 0.18≤T≤1 K: The Binding Energy of H on Liquid ⁴He

M. Morrow, R. Jochemsen, A. J. Berlinsky, and W. N. Hardy

Department of Physics, University of British Columbia, Vancouver, British Columbia V6T 1W5, Canada

(Received 7 November 1980)

Magnetic-resonance studies of the 1420-MHz transition in atomic hydrogen have yielded an accurate value for the binding energy of atomic H on liquid ⁴He. A value of 0.93 ± 0.05 K is derived from two independent determinations of the surface binding: one from the shift in the hyperfine frequency, and the other from the recombination rate. The rate constant for H-H recombination in zero field and the hyperfine frequency of an H atom in the bound surface state have also been determined.

An important consideration in low-temperature experiments with hydrogen atoms is the fact that recombination into H$_2$ molecules is very efficient for H atoms bound to surfaces. The least-binding solid surface, solid H$_2$, has a binding energy of 38 K.[1] Thus at 1 K essentially all of the atoms in a solid H$_2$ container will be bound to the walls. Recombination can be greatly inhibited if the electron spins are polarized by a large magnetic field. However, in order to achieve high degrees of polarization with available laboratory fields, it is necessary to work at temperatures below 1 K. Hence to obtain stabilization of an H-atom gas by spin polarization one must confine the atoms with walls which do not bind a significant fraction of the H atoms at 1 K. Recent magnetic-compression experiments of Silvera and Walraven,[2] of Walraven, Silvera, and Matthey,[3] and of Cline *et al.*,[4] and the zero-field confinement experiments of Hardy *et al.*,[5] have demonstrated that a liquid-⁴He–coated surface satisfies this requirement.

The behavior of the polarized hydrogen gas will depend crucially on the actual binding energy, E_B, of H to the ⁴He surface. At some temperature well below E_B/k_B the surface density will increase rapidly to a value of about 10^{14} cm^{-3}, determined by repulsive H-H interactions.[6,7] Calculations of E_B have been reported by Guyer and Miller,[8] who found $E_B \simeq 0.1$ K for H on ⁴He and by Mantz and Edwards,[9] who found $E_B \geq 0.6$ K. The latter authors emphasized that most of the approximations made in their calculations were expected to lead to an underestimate of E_B.

Very recently Silvera and Walraven[10] have reported an experimental value of 2.5 ± 0.4 K for the binding energy of atomic *deuterium* on liquid ⁴He, based on measurements of recombination rates in an 8-T field. In this Letter we report two essentially independent measurements of E_B for atomic H on ⁴He liquid. One relies on the temperature dependence of the 1420-MHz hyperfine frequency, and the other on the temperature dependence of the recombination rate.

The dilute gas of atomic hydrogen is produced inside an approximately cylindrically shaped Pyrex cell (diameter 1 cm and length 7 cm) by using the techniques described previously[5] but adapted for use in an S.H.E. ³He/⁴He dilution refrigerator. The sealed glass cell is surrounded by a bath of ⁴He liquid which is in thermal contact with the mixing chamber via a sintered copper heat exchanger; the temperatures measured are those of the ⁴He bath. Radio-frequency discharge pulses of duration 50 μs and total energy less than 10^{-3} J are used to produce atoms. The temperature rise is very small and relaxes quickly as measured by both the bath thermometer and the
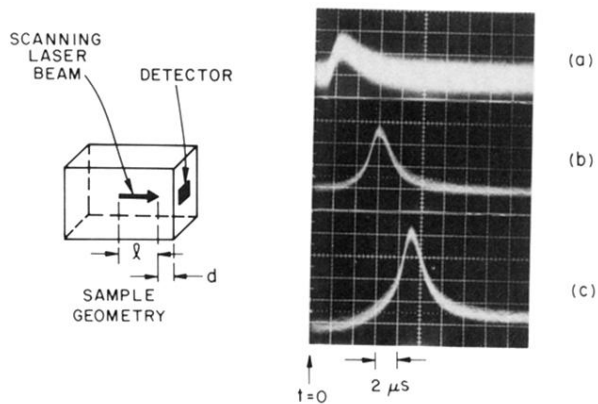
FIG. 2. Schematic on left shows the geometry of the sample. A variable-speed, spinning mirror is used for scanning the laser beam along the sample surface. The laser scanning distance is l and the free propagation distance is d. Photographs show typical pulses for three different scanning velocities: (a) 3.8×10^5, (b) 0.47×10^5, and (c) 0.286×10^5 cm/sec. Time scale is 2 μsec for each large division. The peak arrival times are (a) 2.0 ± 0.2, (b) 5.6 ± 0.2, and (c) 8.9 ± 0.2 μsec.
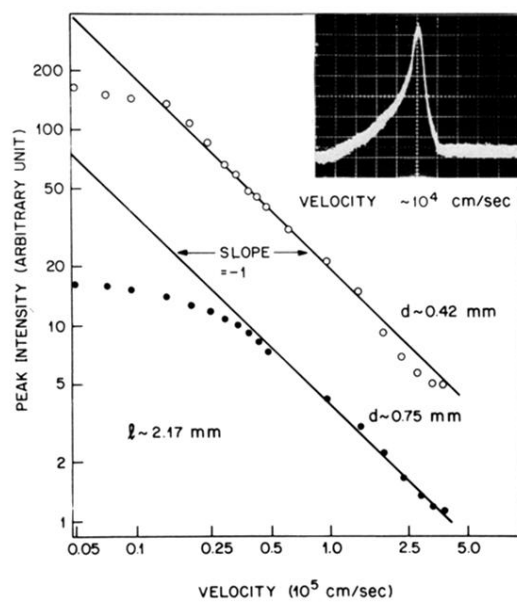
FIG. 4. Peak intensity as a function of scanning velocity for two different distances d and a fixed scanning length l of 2.17 mm. At low velocities attenuation becomes significant, as shown also in the photograph which corresponds to a scanning velocity of 10^4 cm/sec. Time scale is 5 μsec for each large division.